RSC Advances

PAPER

View Article Online
View Journal | View Issue

Cite this: *RSC Adv.*, 2020, **10**, 6146

Argovit™ silver nanoparticles to fight Huanglongbing disease in Mexican limes (*Citrus aurantifolia* Swingle)

José L. Stephano-Hornedo,[ab] Osmin Torres-Gutiérrez,[b] Yanis Toledano-Magaña,[c] Israel Gradilla-Martínez,[d] Alexey Pestryakov,[e] Alejandro Sánchez-González,[b] Juan Carlos García-Ramos *[c] and Nina Bogdanchikova *[d]

Nowadays, Huanglongbing (HLB) disease, commonly known as "yellow dragon disease", affects citrus crops worldwide and has a devastating effect in the agro-industrial sector. Significant efforts have been made to fight the illness, but still, there is no effective treatment to eradicate the disease. This work is the first approach to evaluate the capacity of silver nanoparticles (AgNPs) to directly eradicate the bacteria responsible for Huanglongbing disease, *Candidatus* Liberibacter asiaticus (CLas), in the field. The AgNPs were administered by foliar sprinkling and trunk injection of 93 sick trees with remarkable results. Both methods produce an 80–90% decrease of bacterial titre, quantified by qRT-PCR in collected foliar tissue, compared with the control group. Scanning electron microscopy images show an essential reduction of starch accumulation in phloem vessels after AgNP treatments without evidence of bacteria in the analyzed samples. Compared with other effective methods that involve β-lactam antibiotics, the potency of AgNPs is 3 to 60-times higher when it is administered by foliar sprinkling and from 75 to 750-fold higher when the administration was by trunk-injection. All these results allow us to propose this AgNP formulation as a promising alternative for the treatment of infected trees in the field.

Received 1st November 2019
Accepted 24th January 2020

DOI: 10.1039/c9ra09018e

rsc.li/rsc-advances

1. Introduction

The genus *Citrus* includes several essential crops like oranges, lemons, grapefruit, and limes. They are the world's major fruit crops with global availability and popularity due to their delightful taste, affordable price, and recognized properties for human health (high contents of vitamin C, dietary fibre, amino acids, and fatty acids).[1]

Annual world production of citrus has grown steadily since the late 1990s, with an estimated production of 59 000 000 tons to about 121 000 000 tons in the period 2013–2014. According to the Citrus Fruit Statistics 2015 report published by the Food and Agriculture Organization of the United Nations (FAO), China, Brazil, United States, Mexico, India, Spain, Iran, and Egypt are the main producing countries.[2] Particularly for lemons and limes, the report presented in July 2018 by the Foreign Agricultural Service of the US Department of Agriculture places Mexico as the world-leading producer and exporter.[3]

Despite the promising data in citrus production, the economic impact that Huanglongbing (HLB) disease produces in crops is a big concern in Mexico and the rest of the world. Only in Mexico, where the disease was detected in July 2009, the spread of the disease could produce a 50% decrease in the crop production and a devastating effect in the agro-industrial sector in the worst-case scenario.[4]

Citrus crops are incredibly vulnerable to *Candidatus* Liberibacter asiaticus (CLas), the bacterial agent with high prevalence in Asia and America, and the responsible for Huanglongbing disease.[5] CLas is a Gram-negative phloem-feeding bacteria avoiding the optimal function of roots.[6] The effects in the trees are manifested as defoliation, fruit drop, foliar speckling, asymmetric fruit without juice, and off-flavored, among others.[7] Unfortunately, symptoms are not immediately evident, and they manifest until very advanced stages of the disease.[8]

Many approaches to fight HLB disease have been employed since the beginning of the problem: from the control of the insect vector – *Diaphorina citri* – through the application of insecticides[8] until the use of broad-spectrum antibiotics to overturn the symptoms in diseased trees.[9,10] The best results were obtained with β-lactams and tetracyclines,[10] however, the

[a]*Meredith Gould Laboratories, Tijuana, Baja California, Mexico*
[b]*Facultad de Ciencias, Universidad Autónoma de Baja California (UABC), Carretera Transpeninsular 3917, Ensenada, Baja California 22860, Mexico*
[c]*Escuela de Ciencias de La Salud, Universidad Autónoma de Baja California (UABC), Blvd. Zertuche y Blvd. de los Lagos S/N Fracc. Valle Dorado, 22890 Ensenada, B.C., Mexico. E-mail: juan.carlos.garcia.ramos@uabc.edu.mx*
[d]*Centro de Nanociencias y Nanotecnología, Universidad Nacional Autónoma de México, Km 107 Carretera Tijuana-Ensenada, C.P. 22860, Ensenada, B.C., Mexico. E-mail: nina@cnyn.unam.mx*
[e]*Department of Technology of Organic Substances and Polymer Materials, Tomsk Polytechnic University, Lenin Avenue 30, Tomsk, 634050, Russia*

development of microorganism resistance and the indirect effect on human health is an eminent and growing risk that definitively limits antibiotics use at the field-scale. Actually, there is no chemical or another control method currently available that can completely cure the disease.[11] Therefore, an urgent necessity to find a sustainable solution to treat HLB-infected crops is undeniable.

Silver nanoparticles (AgNPs) emerge as an alternative for the treatment of HLB due to its proven antibacterial activity. Even though its mechanism of action is not completely clear, several reviews agree that cytotoxic and bactericidal activity depends on several physicochemical properties of the nanomaterial such as the size, shape, composition, surface charge, and stability of the suspension they form.[12,13]

These physicochemical features allow particular interactions with the cellular membrane, organelles and specific enzymes and proteins producing different consequences like pits on the membrane, reactive oxygen species overproduction, inhibition of the antioxidant response and other fundamental processes of the bacteria which elicited independently or concomitantly lead to bacterial death.[12,14–18]

In this work, we describe the remarkable results of the commercial formulation of silver nanoparticles (AgNPs) as a bactericidal agent against *Candidatus* Liberibacter asiaticus (CLas). These nanoparticles were administered to HLB-diseased Mexican lime trees (*Citrus aurantifolia* Swingle) through different methods identifying the best of them as well as the effective AgNPs concentration to produce the bactericidal effect.

2. Experimental

2.1 Selection of specimens

For this study, 108 Mexican lime trees (*Citrus aurantifolia* Swingle) of 3 years-old with high rate symptoms of Huanglongbing (HLB) disease were selected from the Valle Viejo orchard, geographically located in the community of Cerro de Ortega, municipality of Tecomán, in the state of Colima, Mexico (Fig. 1). Geographical coordinates: latitude 18.761389°, longitude −103.730556°. The trees were selected during July of 2011 by Roberto Flores Virgen, at the time of the study representative of the State Committee of Phytosanitary Protection of the State of Colima (CESAVECOL) and coordinator of the campaign against HLB disease in the citrus crop in the region.

Fig. 1 Experimental specimens in the Orchard Valle Viejo located in the community Cerro de Ortega, municipality of Tecomán, Colima, Mexico.

Trees used in this study were differentiated from the others with a blue ribbon and the assignation of a code number. From each selected tree, three branches were identified with red ribbons to follow the changes produced with the administration of AgNPs by different routes.

2.2 Physicochemical characterization of Argovit™ AgNPs

Characterization data of the batch used for these experiments was performed by HR-TEM (Jeol JEM-2010 microscope), UV-vis (Agilent Cary 60 spectrophotometer), zeta potential, and hydrodynamic diameter (Malvern, Zetasizer Nano NS DTS-1060) and thermogravimetry (TA Instruments SDT Q6000). Prof. Vasily Burmistrov form Vector-Vita LLC kindly donated silver nanoparticles used in this work. The characterization data provided by Prof. Burmistrov indicate that this AgNPs formulation consists of spheroidal silver nanoparticles with 1.2% (w/w) of metallic silver stabilized with 18.8% (w/w) of polyvinylpyrrolidone (PVP) suspended in water (80% w/w). The size distribution range is 1 to 90 nm, with an average size of 35 ± 7 nm determined by HR-TEM. The hydrodynamic diameter in distilled water is 70 ± 11 nm. Zeta potential of −14 mV and the resonance plasmon on distilled water was registered at 420 nm. The presence of PVP was confirmed by FT-IR.

2.3 AgNPs administration to HLB-infected trees

AgNPs were administered by two routes briefly described in the following paragraphs:

2.3.1 Foliar sprinkling. From a stock solution of Argovit™ (1.2% wt), several dilutions were performed with 0.1% Vatsol OT™ solutions previously prepared with distilled water (Sodium Dioctyl sulfosuccinate, cat no. 44203, Alfa Aesar) to reach final ratios Argovit™ : Vatsol OT™ of 1 : 250; 1 : 1000; 1 : 5000 and 1 : 10 000. The foliar application was carried out with a Shindaiwa (IS726) backpack sprayer with nozzle type D1 (not cat no. its-02-80M, Yamaho) of 0.18 L min^{-1}. The

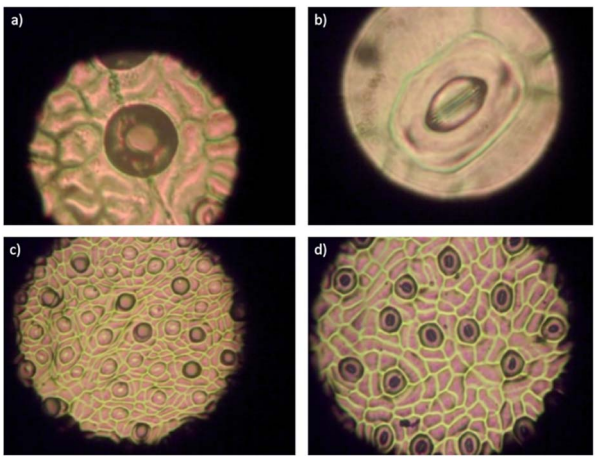

Fig. 2 Microphotographs of Mexican lime (*C. aurantifolia*) stomata. Stomata are opened at 4:00 am ((a) and (c)) and are closed after 9 am ((b) and (d)). Stomata density is 4260 per cm^2, on the undersides of the leaves.

application time was between 4:00 am, and 9:00 am when the stomata are open as shown in Fig. 2.

Administration dates and sample collection post-administration for each experimental group were specified in Table 1. The presence of live and dead bacteria was quantified by qRT-PCR.

2.3.2 Trunk-injection with AgNPs. For trunk-injection, the working solutions were obtained by diluting the AgNPs stock solution with distilled water until the final solutions 1 : 500, 1 : 1000, 1 : 5000, and 1 : 10 000 were obtained. The final solutions were injected into the trees between 9:00 to 13:00 h with the following devices: Quikjet (Arborjet # 070-2250) and XyllaKill (Fig. 3). For trunk injection, two doses of AgNPs was administered to each tree (Table 1) without sample collection after the first administration. Administration and post-administration sample collection were compiled in Table 1.

The Quikjet system for trunk injection requires that three holes (0.93 cm of diameter and 1.5 cm depth) were made in the trunk (Fig. 3a). Each hole is spaced 5 cm from the other in a spiral shape. The holes were sealed with a silicone septum. The required volume of the AgNPs solution was applied through the silicone septum with manual pressure.

The XyllaKill device (Fig. 3b) also requires the perforation on the trunk; however, in this case, the tip of the device is directly adjusted to the hole for the administration of the substance. In a few hours, the entire volume of the vessel (in this case AgNPs) enters by gravity in a passive way. The vessel is reusable, the cylinder contains 20 mL and can be refilled as many times as needed without removing the device. For this work, two XyllaKill devices were mounted in each treated tree. Both devices work at the same time to administer a final volume of 40 mL to each treated tree, which corresponds to one dose of the treatment.

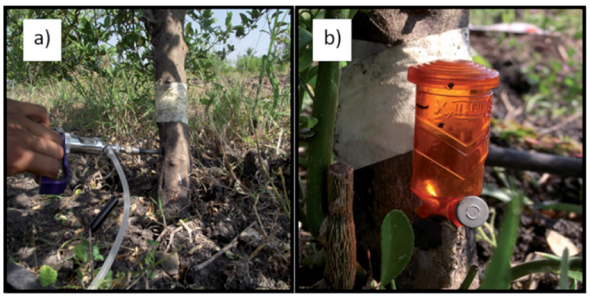

Fig. 3 Devices employed for AgNPs administration (a) Quikjet and (b) XyllaKill.

2.4 Sampling of plant material

From the 108 specimens used in this study, three branches identified with a red ribbon were used to collect samples for qPCR (two branches) and electron microscopy (one branch). Ten mature leaves were collected from each branch before and after the administration of AgNPs. The before-administration

Table 1 AgNP application scheme to Mexican limes infected with Huanglongbing. Application and sample collection dates, the volume applied and the corresponding silver amount[a]

Dilution	# trees	Application dates	Sample collection post	Total vol/tree (mL)	[Ag]/tree (mg)	[Ag]/tree (μmol)
Foliar sprankling						
1 : 250	6	29 oct	8 nov	2000	96	890.0
	6	29 oct/11 nov	25 nov	4000	192	1780.0
	6	29 oct/11 nov/27 nov	7 dic	6000	288	2670.1
1 : 1000	6	30 oct	8 nov	2000	24	222.5
	6	30 oct/11 nov	25 nov	4000	48	445.0
	6	30 oct/11 nov/27 nov	7 dic	6000	72	667.5
1 : 5000	6	30 oct	8 nov	2000	4.8	44.5
	6	30 oct/11 nov	25 nov	4000	9.6	89.0
	6	30 oct/11 nov/27 nov	7 dic	6000	14.4	133.5
1 : 10 000	6	31 oct	8 nov	2000	2.4	22.2
Control	8	—	7 dic			
Trunk injection HyllaKill method						
1 : 500	5	5 aug/10 aug	17 aug	80	19.2	178
1 : 5000	5	7 aug/10 aug	17 aug	80	1.92	17.8
1 : 10 000	3	8 aug/10 aug	17 aug	80	0.096	0.89
Trunk injection Quikjet method						
1 : 500	5	5 aug/8aug	17 aug	30	0.72	6.6
1 : 1000	5	7 aug/8aug	17 aug	30	0.36	3.3
1 : 5000	5	7 aug/8aug	17 aug	30	0.072	0.66
1 : 10 000	5	8 aug/10 aug	17 aug	30	0.036	0.33
Control	7	—	17 aug	—	—	

[a] A 1 : 1000 dilution correspond to 12 μg of metallic silve per mL of formulation.

samples were collected within the 18-29th July 2011. Dates of the post-administration collections are compiled in Table 1. The collected samples were kept in sealed bags separately within a cooler to 4 °C, transported immediately to the laboratory for qPCR procedure.

The leaves were cleaned with 70% alcohol and blotting paper; after that, were finely minced with a double edge knife, and 40 mg of this material was deposited within a microtube. Four microtubes per sample were prepared, two samples were identified with the branch and tree code, the other two with the same code plus EMA.

Samples from the third branch were kept in sealed bags separately and within a cooler at 4 °C and processed following the glutaraldehyde-osmium tetroxide protocol. Once processed, samples were storage with desiccant and transported to the nano-characterization unit of CNyN-UNAM. Samples were processed at high-vacuum and coated with gold following standard sample preparation procedure. Images were obtained with a JEOL JMS-5300.

2.4.1 EMA pre-treatment. For differentiation of DNA extracted from live and dead bacteria, we use Ethidium bromide monoazide (EMA, Invitrogen, E1374). This reagent inhibits the amplification of DNA through a covalent binding promoted by photoactivation. The selectivity is because the agent can only reach the DNA of dead cells with the damaged membrane.[19,20] Therefore, all microtubes that come from the previous step marked with the EMA code containing the samples of mature leaves of the two branches of the experimental specimens were pretreated before proceeding to DNA extraction. Briefly, samples were homogenized with a TissueLyser (30 Hz, 2 min). After that, 25 μL of EMA was added at dark, mixing softly still in darkness, each minute for 5 min. Later, microtubes opened over ice (to avoid overheat) were exposed for 1 min to a 600 W halogen bulb placed 15 cm above. The mixture was centrifuged at 5000*g* for 5 min and the supernatant discarded. The obtained pellet was used to extract DNA as described below.

2.5 DNA extraction from live and dead bacteria

The DNA extraction was performed following the standardized protocol from Laboratorio de Diagnóstico del Centro Nacional de Referencia de Control Biológico (CNRCB-SENASICA). Briefly, 275 μL of PBS and 150 μL of C-L buffer were added to each microtube containing 40 mg of tissue. The mixture was homogenized with a TissueLyser LT (Qiagen, Germany) using tungsten carbide beads. Purification of DNA was performed with the AxyPrep Multisource Genomic DNA Miniprep Kit (AP-MN-MS-GDNA-50, Axygen). The purity of the extracted rDNA was determined by spectrophotometric measurements (260/280 ratio, Nanodrop 2000), then the samples were quantified and preserved at −20 °C until their use.

2.6 Real-time PCR

Real-time qPCR was performed in the Genomic Core Center for AIDS Research (CFAR) Stein Clinical Service, UCSD, La Jolla, San Diego, CA. 92093 in an Applied Biosystems 7500 equipment. Most of the DNA samples were adjusted to 20 ng μL^{-1} (with and without EMA); in some cases, was necessary the adjustment to 10 ng μL^{-1}. The reaction was performed in Multiplex way, simultaneous amplification of the 16S ribosomal gene of CLas, three genes per bacteria,[21,22] using the primers

HLBp: 5′ 6FAM/AGA CGG GTC AGT AAC GCG/3′BHQ-1

HLBas: TCG AGC GCG TAT GCA ATA CGC

HLBr: CGC TTA TCC CGT AGA AAA AGG TAG

The reaction mixture contains 2 μL of citrus DNA (20 ng μL^{-1}), 10 μL TaqMan Universal PCR Master Mix (2X), 1 μL of primers (20X, TET) and 7 μL of free-nucleases water to get a final volume of 20 μL. The amplification program employed was a denaturalizing initial step of 95 °C for 15 minutes, followed by 40 cycles of 94 °C for 15 seconds and 58 °C for 1 minute.

2.6.1 Quantification of *Candidatus* Liberibacter asiaticus (CLas). A standard curve was obtained with the synthetic 16S gen (280.95 ng μL^{-1}):

5′ GTC GAG CGC GTA TGC AAT ACG AGC GGC AGA CGG GTG AGT AAC GCG TAG GAA TCT ACC TTT TTC TAC GGG ATA ACG CA3′

The cycle threshold, C_t, was obtained from the standard curve as follows: $y = -3.5031x + 39.7609$; $R^2 = 0.9996$. Formula for determining bacterial titre $[\text{CLas}] = 10^{\{(C_t - 39.7609)/-3.5031\}}$ The [CLas] for each experimental sample were determined by interpolation of their C_t values.

2.7 Statistical analysis

A non-parametric *U*-test Mann–Whitney was performed to determine the significant differences ($p < 0.05$) between AgNPs treatments with control groups and between treatments.

3. Results and discussion

The characterization of the AgNPs batch employed in this work shows that the properties of nanomaterials agree with data provided by the supplier. We found semi-spherical nanoparticles with a distribution range of 3 to 96 nm and an average size of 32.98 ± 22.33 nm. TEM images at different magnifications and size histograms are shown in Fig. 4. The resonance plasmon in water was observed at 429 nm, while zeta potential and hydrodynamic diameter found in the same solvent were −1.48 mV and 121 nm, respectively. The formulation composition was evaluated by TGA showing 77.25% of water, 21.52% of PVP, and 1.23% of silver. The polymer was identified by its decomposition temperature (446 °C). A summary of characterization performed is shown in Fig. 4.

In this work, 93 HLB-infected trees were treated with a commercial formulation of AgNPs. The elimination of CLas from infected *Citrus aurantifolia* Swingle trees was determined by qRT-PCR quantifying the number of live and dead bacteria in 40 g of tissue collected nine days after the administration of

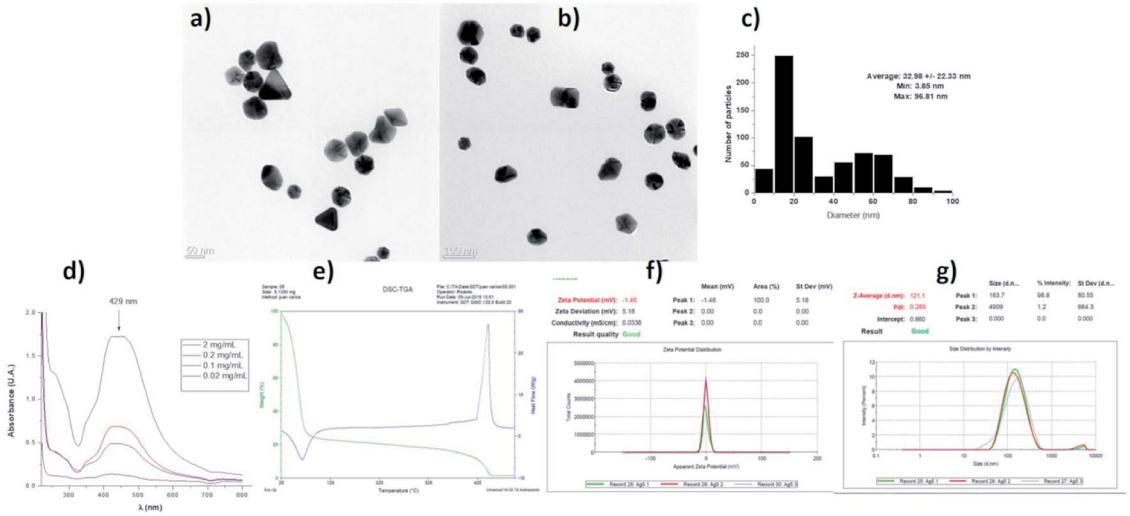

Fig. 4 Characterization of AgNP used batch. AgNPs used in this work were characterized by HR-TEM (a and b) and the distribution histogram is presented in (c). Plasmonic resonance by UV-vis (d), thermogravimetric analysis (e), zeta potential (f) and hydrodynamic diameter (g) were also determined.

AgNPs treatment concluded. Table 2 contains the average of CLas present in tissue expressed in logarithmic units (log CLas) and the corresponding bacterial elimination effectiveness. These data were normalized to control group.

Data from foliar application shows that CLas elimination effectiveness does not show a dose–dependent behaviour for these AgNPs (Table 2, Fig. 5). The highest concentration employed (1 : 250 dilution) only reach a decrease of the

Table 2 Elimination effectiveness of AgNPs. Average of live bacteria quantified in 40 g of tissue obtained before and after AgNPs administration through different methods, and the bacterial elimination effectiveness derived from these data

Dilution	[Ag]/tree (mg)	[Ag]/tree (μmol)	Mean live CLas (log[CLas] before)	Mean live CLas (log[CLas] after)	Effectiveness[a]%
Foliar spranking					
1 : 250	96	890.0	4.65	4.36	67.36
	192	1780.0	4.68	4.62	43.29
	288	2670.1	4.75	4.63	52.55
1 : 1000	24	222.5	4.62	3.80	90.31
	48	445.0	4.91	4.17	88.25
	72	667.5	4.85	4.44	75.24
1 : 5000	4.8	44.5	4.62	4.38	63.27
	9.6	89.0	4.46	4.98	−108.55
	14.4	133.5	4.51	4.97	−82.77
1 : 10 000	2.4	22.2	4.75	4.84	−16.56
Trunk injection HyllaKill method					
1 : 500	19.2	178	4.08	3.73	71.44
1 : 5000	1.92	17.8	4.56	3.99	82.86
1 : 10 000	0.096	0.89	4.26	3.89	72.76
Trunk injection Quikjet method					
1 : 500	30	0.72	4.23	4.13	49.64
1 : 1000	30	0.36	4.20	4.00	60.04
1 : 5000	30	0.072	3.94	3.68	65.38
1 : 10 000	30	0.036	4.33	3.98	71.11
Control	—	—	4.28	4.42	0
PS-5	—	—	6.03	4.89	93
Cre-nano	—	—	6	2	99

[a] Values were normalized respect bacterial proliferation on control groups. PS-5 = 5 g (13.4 mmol) of penicillin G potassium salt + 0.5 g (0.859 mmol) of streptomycin in 100 mL of water per tree. Cre-nano = nano formulation with sodium ampicillin (1000 mg L^{-1}; 2.69 mM). 500 mL by bark application equivalent to 1.345 mmol per tree.

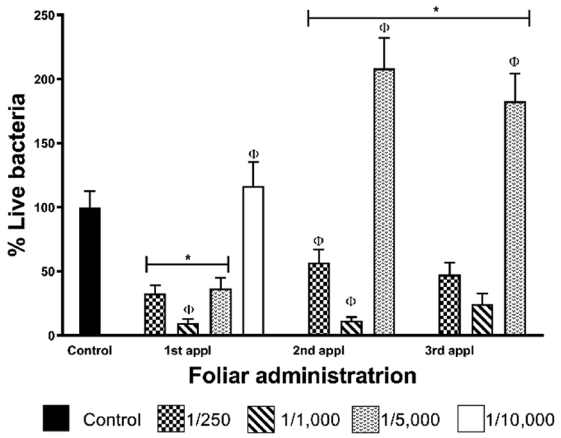

Fig. 5 Bacterial elimination effectiveness after foliar administration of a commercially available AgNPs formulation. Collection of leaves samples to quantify the bacterial titer was nine days after the administration of AgNPs. All data were normalized respect control group. 20% AgNPs solution was employed to prepare the final dilution employed: 1 : 250, 1 : 1000, 1 : 5000 and 1 : 10 000. * and Φ represent statistically significant difference compared with control and between AgNPs used concentrations, respectively.

bacterial titre of 68% and 44% after the first and second applications, respectively. Interestingly, the best bacterial elimination effect was found with the AgNPs dilution of 1 : 1000, that after the first administration reduces in 90% the bacterial titre in leaves. The concentration of metallic silver that produces 90% of bacterial titre reduction is 24 mg per tree that corresponds to 222 μmol of Ag per tree. Practically the same effect was observed after the second administration (88% decrease of bacterial titre), but the effectiveness decreases after the third dose with a bacterial titre of 35% compared with the control group. The rest of the dilutions assayed do not present a favourable response after the first administration. These results also allow us to propose a most frequent AgNPs administration scheme not only to avoid reach bacterial typical proliferation rate for the season as shown in this work but also to achieve the complete elimination of the bacteria.

Effectiveness decrease of AgNPs 1 : 1000 dilution could be associated with several factors related to the foliar application such as low absorbance of AgNPs by leaves, loss of compounds by wind-drag, decomposition of AgNPs or oxidation of silver by UV, among others. However, despite the effectiveness reduction at the third administration, it is evident that the effect on the bacterial titre just after the AgNPs administration. For dilution 1 : 250, the aggregation and, in turn, the lower availability of AgNPs for the leaves could be the reason for the low bacterial elimination effectiveness (Fig. 5). The rest of the concentrations employed are too diluted to show a reasonable effect by this administration method.

Although we could not reach the complete elimination of the bacteria with the three-dose AgNPs administration scheme, one dose every seven days, it is essential to remark that AgNPs dilution of 1 : 1000 reduces 90% the bacterial titre after the first administration (Fig. 5). This result is very significant due to AgNPs administration was carried out in the season where the largest population of live bacteria was quantified in the leaves of infected trees of the region.[23]

On the other hand, to avoid the problems derived from the foliar sprinkling (low absorption, photo-oxidation, wind-drag) and enhance the effect of AgNPs, the trunk-injection was explored. With this method, the applied volume was reduced 25-times and at least 5-fold lower concentrations were used (Table 2). By trunk-injection, the nanoparticles are not exposed to sunlight, and the absorption is secured. Two injection methods were employed, one commercial (Quickjet) and a home-made dispositive (XyllaKill). The former injects with an air hydraulic system, the latter by gravity.

The compressed-air-assisted injection of AgNPs shows an inverse dependence between the bacterial titre decrease and the concentration of active compound administered. The elimination effectiveness of this method is in the range of 49–71% (Fig. 6a). All the concentrations assessed exhibit a bacterial titre decrease with a statistically significant difference compared with the control.

Meanwhile, bacterial elimination effectiveness of gravity trunk-injection (XyllaKill method) does not show a dose–dependence behaviour, but a considerable decrease within the range of 72–83% was observed (Fig. 6b). All concentrations showed significant efficacy in bacterial elimination, and, despite it is not statistically significant, the middle concentration of the three assessed showed the highest capacity to decrease bacterial titre, just as seen for the foliar sprinkling.

It seems that the combination of high pressure and high concentration produces a not favourable effect on the bacterial elimination effectiveness of AgNPs. The 1 : 500 dilution of AgNPs injected by gravity reach elimination of 80%, while the same dose with the compressed-air system (Quickjet) only reached 50%. The activity loss could be associated with the agglomeration of nanoparticles facilitated by the pressure of compressed air employed and high AgNPs concentration.

Xyllakill method shown that small concentrations of the active component, such as 1.92 mg of metallic Ag per tree (17.8 μmol metallic Ag per tree) injected by gravity, produce

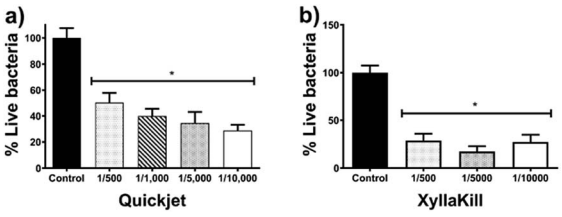

Fig. 6 Bacterial elimination effectiveness after trunk-injection of a commercially available AgNPs formulation administered with (a) XyllaKill and (b) Quickjet. A 20% AgNPs stock solution was employed to prepare the final dilution employed: 1 : 500, 1 : 1000, 1 : 5000 and 1 : 10 000. Collection of leaves samples to quantify the bacterial titer is described in the experimental section. All data were normalized respect control group. * and Φ represent statistically significant difference compared with control and between AgNPs used concentrations, respectively.

a bacterial titre reduction of 80%. The metallic silver employed with this method is 12.5-times lower than that employed to produce a similar decrease by foliar sprinkling, besides the volume also is reduced 25-times.

To evaluate the effect of AgNPs treatments, we explored the changes in phloem vessels and starch accumulation within them, the latter identified as a critical factor in the development of adverse effects of CLas infected trees. Images in Fig. 7a–c show the unobstructed phloem vessels of healthy trees and the absence or minimum presence of starch within. On the other hand, infected trees present deformed and starched vessels (Fig. 7f–i). Fig. 7f shows starching of vessels, indicative of an advanced stage of disease in the tree. Live and dead bacteria present on infected trees are shown in Fig. 7d and e.

Fig. 7j–l shows the appearance of collected samples after trunk-injection of AgNPs dilution 1 : 500, while Fig. 7m–o present the effect after trunk-injection administration of AgNPs dilution 1 : 10 000. In this representative sample of collected images, no bacteria were found; vessel deformation still present but starch accumulation is lower than that observed on infected trees. Although images do not show dramatic changes in vessel morphology, the absence of bacteria in the examined samples and decrease of starch accumulation suggest an essential effect of AgNPs after a short time after the administration.

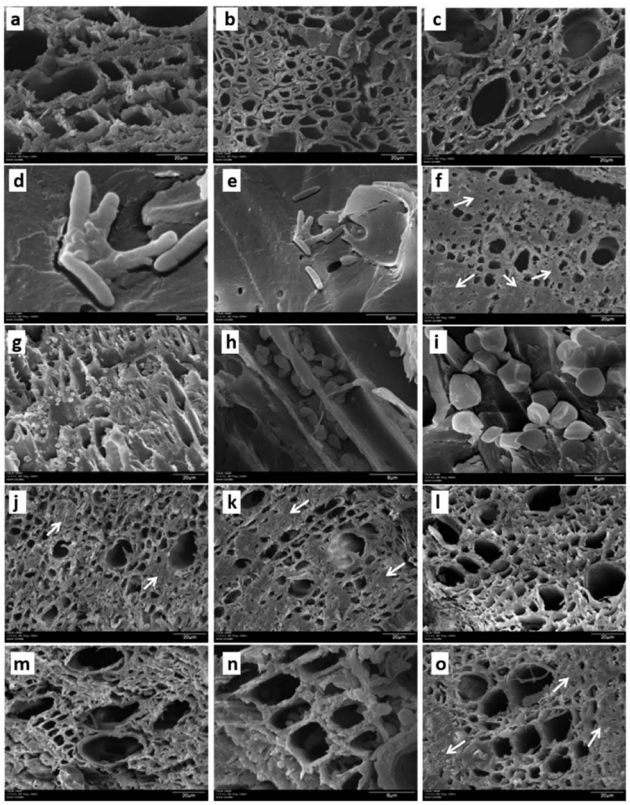

Fig. 7 Scanning electron microscopy images of leaves and branches of healthy trees (a–c), HLB-infected (d–i) and HLB-infected trees treated with AgNPs (j–n). Images (d) and (e) show the bacteria observed in HLB-infected trees. White arrows indicate deformed or blocked vessels. Starch accumulation in HLB-infected trees is shown with different magnifications and cuts at (g) cross-section, (h) longitudinal cut and (i) amplification of the latter. Images (j–l) and (m–o) show cross-sections of trunk-injected trees with AgNPs diluted 1 : 500 and 1 : 10 000, respectively. Images (k) and (n) show starch accumulation after the respective AgNPs treatment.

The complete characterization and the quantification of metallic silver in our AgNPs formulation allow establishing a direct comparison of the active substance employed in this work with other methods proposed to combat HLB disease. In any of the results described including our work, no complete elimination of bacteria is achieved. Foliar application of AgNPs needs 30 to 60-times lower concentration of active component to produce a similar effect that penicillin G and 3 to 6-times compared with sodium ampicillin.[24,25]

On the other hand, considering the metallic silver (17.8 μmol metallic Ag per tree) employed by trunk injection, concentrations of the antibiotics are almost 750-times higher for penicillin G (13.4 mmol) and 75-times for sodium ampicillin (1.34 mmol of the antibiotic per tree). The advantages and disadvantages of administration pathways must play an essential role in the selection of effective treatment; however, it is undeniable that the concentration of the active substance is a predominant factor for the selection and this AgNPs formulation is a most potent agent than β-lactam antibiotics to decrease the bacterial titre in the tree.

It is important to remark that even with foliar sprinkling, the bacterial growth-inhibitory potency of AgNPs is higher than that observed for antibiotics, because bacterial titre decrease (superior to 85%) was observed with 3-to-30-times lower concentration of the active compound than for ampicillin and penicillin G, respectively (Table 2, foliar sprinkling, AgNPs dilution 1 : 1000).

Results discussed above acquire even more importance due to the β-lactam antibiotics have been classified as a contamination potential hazard of food plants by the Environmental Protection Agency (EPA).[26] In addition, there is a reduced bactericidal activity for streptomycin alone against CLas determined in an *in vitro* model, one of the components of the most effective antibiotic formulations.[27] Therefore, despite its high efficacy against CLas on infected trees, the use of these antibiotics, alone or in a mixture, does not appear to be a feasible alternative for the treatment of HLB.

The antibacterial activity against CLas of AgNPs could be produced by the same mechanism of action that one observed in other Gram-negative bacteria like *Escherichia coli*,[28] fungi such as *Cladosporium cladosporiorides* and some *Penicillium* spp.,[29] found as contaminants in vanilla (*Vanilla planifolia* Jacks. ex Andrews). The bacterial contamination was eliminated on vanilla plantlets with concentrations of 25 and 50 mg L^{-1} of AgNPs. The explants were exposed by 42 days to the culture media containing AgNPs without evidence of cytotoxicity or genotoxicity despite the long exposure time.

The proposed antimicrobial effect was through interaction with the cellular membrane of the microorganism and induction of redox unbalance by the increase of ROS concentration within it.[28,29] Internalization of silver nanoparticles within bacteria depends, among other factors, of its size and surface charge. For both Gram-positive and Gram-negative bacteria,

smallest AgNPs have more significant the bactericidal effect, and the surface charge allows or inhibits the approach of AgNPs to the bacterial membrane.[30] Besides the modification of surface charge, the use of different molecules as coating agents provide a wide range of stability. This stability furnishes a differential bactericidal activity but also decreases the higher toxicity that silver ions own,[13] an important reason to prefer AgNPs formulation instead a direct silver ions sources like $AgNO_3$ or silver acetate. It is known the effect of silver ions on the destabilization of cellular membrane, its interaction with enzymes and proteins (especially with those containing thiol groups and ribosomal), nucleic acids (particularly with pyrimidine bases), and overproduction of reactive oxygen species (ROS) within the cell.[30]

On the other hand, despite the proposal that AgNPs only function as Ag^+ ions container, several works showed that the effect exerted by intact AgNPs must be considered.[31–33] The differential response elicited by AgNPs but not by Ag^+ involves the specific upregulation genes involved in plant defense system of *Arabidopsis thaliana*,[31] the higher phytotoxicity on the common grass (*Lolium multiflorum*) that cannot be decreased by thiol compounds[32] or different neurotoxicity pathways on *Pimephales promelas*.[33] Therefore, the generalization of the cytotoxic, genotoxic, and phytotoxic response of AgNPs must be avoided, and each nanoparticle formulation considered as a particular species.

In this sense, the AgNPs formulation used in this work has been evaluated in other plants with encouraging results. Concentrations of 50 mg L^{-1} of Argovit™ AgNPs (27.8 μM of metallic silver) or a lower concentration produce beneficial effects on vanilla and sugarcane, *i.e.* hormetic effect triggered by ROS increase, shoot multiplication rate, increase of macro- and micronutrients within vegetal cells, among others.[29,34] In the case of vanilla, the beneficial effects with low AgNPs concentrations were obtained without compromising the mitotic index or generating chromosomic aberrations that could lead to genotoxic damage.[35] Recent work describes the transport and accumulation of Argovit™ on stevia (*Stevia rebaudiana* B.), taking advantage of the fluorescence showed by AgNPs and not presented by the silver ions. In this report, Bello–Bello and co-workers also identified the concentration of 50 mg L^{-1} of AgNPs as beneficial for stevia and observed a decrease in number and length of shoots with concentrations of 100 and 200 mg L^{-1}. The accumulation of AgNPs on the stevia stem and leaves increase with the concentration of AgNPs added to the culture medium. It is important to note that a 4.5-fold increase of Ag was found on plants exposed to 100 g L^{-1} compared with those exposed to 50 mg L^{-1} of AgNPs (determined by ICP-MS), making clear the Ag accumulation dependence with the concentration. The authors propose the xylem and plasmodesmata as the most important vehicles in the distribution and translocation of AgNPs.

The distribution and translocation pathways proposed by Bello–Bello and co-workers suggest and important biodistribution on stevia. This biodistribution could be expected on HLB-infected trees treated with AgNPs, allowing that AgNPs reach whole infected stem and leaves on the tree, decreasing the bacterial titre and reducing the starch accumulation observed in the micrographs of Fig. 7. Further experiments must be performed to determine the fate of total silver, as AgNPs or silver ions, not only in the tree (fruits, stem, leaves, roots) but in the surrounding soil. It should be considered that the large amount of PVP (Ag : PVP; 6 : 94) in the formulation evaluated in this work could give it superior stability throughout time and biotransformation in diverse environments compared with other uncoated formulations or those AgNPs formulations coated with a smaller amount of polymer or stabilizing agent.

The same beneficial effects observed for vanilla, sugarcane, and stevia, besides the distribution behaviour of AgNPs observed on stevia are expected for lime trees exposed to low concentrations of Argovit™. This effect could help in crop recovery once the bacterial contamination has been eliminated and prevent the new infection. Further experiments must be done to identify the possible hormetic effect of AgNPs in lime trees, increase the frequency of the identified sufficient concentrations to achieve the completeness of bacterial elimination and exploration of the biodistribution pathways. Also, additional experiments to determine the fate of the AgNPs. However, these results have shown the superior potency of AgNPs to eliminate the bacterial agent responsible for Huanglongbing disease, *Candidatus* Liberibacter asiaticus, directly in affected trees, results only achieved by β-lactam antibiotics, a non-recommendable option for crop protection. In summary, AgNPs formulation Argovit™ represents a new alternative for the treatment of Huanglongbing disease, that tremendously affects the citrus crops.

Currently, we started a study for the evaluation of the fate and speciation of silver within the infected HBL-tree and the surrounding soil throughout three years long. During this study several samples of different parts of the tree and surrounding soil will be collected through time two times per season to evaluate the antioxidant response of the trees and its effect on the fruit development besides the quantification and quantification of silver on each part.

4. Conclusions

As far as we know, this is the first approach to evaluate the antibacterial potency of AgNPs against Gram-negative bacteria *Candidatus* Liberibacter asiaticus in the field. Our results showed the effectiveness of AgNPs to inhibit the proliferation bacteria responsible for the Huanglongbing disease, commonly known as "yellow dragon disease" that affects citrus crops worldwide, with both administration methods assessed: foliar sprinkling and trunk-injection.

Both assayed administration methods have shown remarkable bacterial titre decrease after a short administration scheme. Three doses of AgNPs administered by foliar sprinkling produce a reduction of the bacterial titre of 90%. On the other hand, AgNPs trunk-injection with 12.5-times lower concentration than that used for foliar sprinkling, and 25-fold lower volume reached 80% of bacterial titre decrease. Scanning electron microscopy images confirm the bacterial elimination with AgNPs treatment and show a significant decrease in starch

accumulation within phloem vessels compared with HLB-infected trees.

The effectiveness of AgNPs to inhibit bacterial growth in citrus trees is comparable to that observed for the most effective systems studied directly on diseased trees, ampicillin, and a mixture of penicillin G + streptomycin. However, the potency of this AgNPs formulation by trunk injection is 75 to 750 times higher than that found for penicillin G and sodium ampicillin. These results allow us to conclude that AgNPs administered by gravity trunk injection is the best option to reduce CLas bacterial titer.

The antibacterial potency found for this AgNPs formulation at a minimal concentration and short exposure time could represent a real alternative for a still unsolved problem, the treatment of infected-HLB trees. We are currently working on the identification of final fate and the speciation of silver within the infected tree and the surrounding soil on a three years long experiment to complete the effects profile due to an AgNPs long-time exposure.

Conflicts of interest

The authors declare no conflict of interest.

Acknowledgements

The research was funded by CONACYT 293418 (Red Internacional de Bionanotecnología) and Tomsk Polytechnic University Competitiveness Enhancement Program (project VIU-ISHBMT-65/2019). Authors thank the invaluable support of the State Committee of Phytosanitary Protection of the State of Colima (CESAVECOL), especially to Roberto Flores Virgen. The authors thank the Genomic Core Center for AIDS Research (CFAR) Stein Clinical Service, UCSD, for the support and technical assistance in the real-time PCR determinations. J. C. G. R. and Y. T. M. thank CONACYT 294727 (Red Farmoquímicos) for student mobility.

References

1 Y. Liu, E. Heying and S. A. Tanumihardjo, *Compr. Rev. Food Sci. Food Saf.*, 2012, **11**, 530–545.
2 Food and Agriculture Organization of the United Nations, *Citrus Fruits Statistics 2015*, Rome, 2016.
3 United State Department of Agriculture Foreign Agricultural Services, *Citrus: World Markets and Trade*, 2018, pp. 1–11.
4 D. Salcedo, G. Mora, I. Covarrubias, C. Cíntora, F. DePaoilis and S. Mora, *Comunnica Magazine*, 2011, pp. 40–47.
5 T. R. Gottwald, *Annu. Rev. Phytopathol.*, 2010, **48**, 119–139.
6 E. G. Johnson, J. Wu, D. B. Bright and J. H. Graham, *Plant Pathol.*, 2014, **63**, 290–298.
7 F. Martinelli and A. M. Dandekar, *Front. Plant Sci.*, 2017, **8**, 904.
8 J. A. Tansey, P. Vanaclocha, C. Monzo, M. Jones and P. A. Stansly, *Pest Manage. Sci.*, 2017, **73**, 904–916.
9 D. R. Boina and J. R. Bloomquist, *Pest Manage. Sci.*, 2015, **71**, 808–823.
10 R. A. Blaustein, G. L. Lorca and M. Teplitski, *Phytopathology*, 2018, **108**, 424–435.
11 J. M. Bové, *J. Plant Pathol.*, 2006, **88**, 7–37.
12 C. Levard, E. M. Hotze, G. V. Lowry and G. E. Brown, *Environ. Sci. Technol.*, 2012, **46**, 6900–6914.
13 S. Ahlberg, A. Antonopulos, J. Diendorf, R. Dringen, M. Epple, R. Flöck, W. Goedecke, C. Graf, N. Haberl, J. Helmlinger, F. Herzog, F. Heuer, S. Hirn, C. Johannes, S. Kittler, M. Köller, K. Korn, W. G. Kreyling, F. Krombach, J. Lademann, K. Loza, E. M. Luther, M. Malissek, M. C. Meinke, D. Nordmeyer, A. Pailliart, J. Raabe, F. Rancan, B. R. Rothen-Rutishauser, E. Rühl, C. Schleh, A. Seibel, C. Sengstock, L. Treuel, A. Vogt, K. Weber and R. Zellner, *Beilstein J. Nanotechnol.*, 2014, **5**, 1944–1965.
14 C. Liao, Y. Li and S. C. Tjong, *Int. J. Mol. Sci.*, 2019, **20**(2), 449.
15 V. Pareek, R. Gupta and J. Panwar, *Mater. Sci. Eng., C*, 2018, **90**, 739–749.
16 A.-C. Burduşel, O. Gherasim, A. M. Grumezescu, L. Mogoantă, A. Ficai and E. Andronescu, *Nanomaterials*, 2018, **8**, 681.
17 R. Foldbjerg, X. Jiang, T. Miclăuş, C. Chen, H. Autrup and C. Beer, *Toxicol. Res.*, 2015, **4**, 563–575.
18 A. Yan and Z. Chen, *Int. J. Mol. Sci.*, 2019, **20**, 23–25.
19 P. Trivedi, U. S. Sagaram, J. S. Kim, R. H. Brlansky, M. E. Rogers, L. L. Stelinski, C. Oswalt and N. Wang, *Eur. J. Plant Pathol.*, 2009, **124**, 553–563.
20 K. Rudi, B. Moen, S. M. Drømtorp and A. L. Holck, *Appl. Environ. Microbiol.*, 2005, **71**, 1018–1024.
21 W. Li, J. S. Hartung and L. Levy, *J. Microbiol. Methods*, 2006, **66**, 104–115.
22 J. S. Kim and N. Wang, *BMC Res. Notes*, 2009, **2**, 2–5.
23 J. A. López-Buenfil, J. A. Ramírez-Pool, R. Ruiz-Medrano, M. del C. Montes-Horcasitas, C. Chavarin-Palacio, J. Moya-Hinojosa, F. J. Trujillo-Arriaga, R. Lira-Carmona and B. Xoconostle-Cázares, *Pak. J. Biol. Sci.*, 2017, **20**, 113–123.
24 M. Zhang, C. A. Powell, L. Zhou, Z. He, E. Stover and Y. Duan, *Phytopathology*, 2011, **101**, 1097–1103.
25 C. Y. Yang, C. A. Powell, Y. P. Duan and M. Q. Zhang, *Plant Dis.*, 2016, **100**, 2448–2454.
26 Food and Drug Administration, *Draft Guidance for Industry: Hazard Analysis and Risk-Based Preventive Controls for Human Food*, 2018, FDA-2016-D-2343.
27 M. Zhang, Y. Guo, C. A. Powell, M. S. Doud, C. Yang and Y. Duan, *PLoS One*, 2014, **9**, 17–21.
28 R. Vazquez-Muñoz, B. Borrego, K. Juárez-Moreno, M. García-García, J. D. Mota Morales, N. Bogdanchikova and A. Huerta-Saquero, *Toxicol. Lett.*, 2017, **276**, 11–20.
29 J. L. Spinoso-Castillo, R. A. Chavez-Santoscoy, N. Bogdanchikova, J. A. Pérez-Sato, V. Morales-Ramos and J. J. Bello-Bello, *Plant Cell, Tissue Organ Cult.*, 2017, **129**, 195–207.
30 A. Kedziora, M. Speruda, E. Krzyzewska, J. Rybka, A. Lukoviak and G. Bugla-Ploskonska, *Int. J. Mol. Sci.*, 2018, **19**, 444.
31 R. Kaveh, Y.-S. Li, S. Ranjbar, R. Tehrani, C. L. Brueck and B. Van Aken, *Environ. Sci. Technol.*, 2013, **47**, 10637–10644.

32 L. Yin, Y. Cheng, B. Espinasse, B. P. Colman, M. Auffan, M. Wiesner, J. Rose, J. Liu and E. S. Bernhardt, *Environ. Sci. Technol.*, 2011, **45**, 2360–2367.

33 N. García-Reyero, A. J. Kennedy, B. L. Escalon, T. Habib, J. G. Laird, A. Rawat, S. Wiseman, M. Hecker, N. Denslow, J. A. Steevens and E. J. Perkins, *Environ. Sci. Technol.*, 2014, **48**, 4546–4555.

34 J. J. Bello-Bello, R. A. Chavez-Santoscoy, C. A. Lecona-Guzmán, N. Bogdanchikova, J. Salinas-Ruíz, F. C. Gómez-Merino and A. Pestryakov, *Dose-Response*, 2017, **15**, 1–9.

35 J. Bello-Bello, J. Spinoso-Castillo, S. Arano-Avalos, E. Martínez-Estrada, M. Arellano-García, A. Pestryakov, Y. Toledano-Magaña, J. García-Ramos and N. Bogdanchikova, *Nanomaterials*, 2018, **8**, 754.